

## Existence Field of the $\sigma$ Phase of the Co–Cr–Ni–V Quaternary at 800°C

E. G. Kabanova, G. P. Zhmurko, V. N. Kuznetsov, and A. V. Leonov

Department of General Chemistry  
e-mail: kabanova@general.chem.msu.ru

Received March 31, 2008

**Abstract**—We studied phase equilibria in the Co–Cr–Ni–V system at 800°C by means of microstructure examination, X-ray powder diffraction, and electron probe microanalysis. We also constructed sections through the Co–Cr–Ni–V isothermal tetrahedron containing 10 and 20 at % vanadium.

**DOI:** 10.3103/S0027131408060084

Nickel and cobalt base alloys doped with chromium and vanadium are widely used as refractory construction materials. During long-term performance at high temperature, however, a  $\sigma$  phase, which has high brittleness and hardness, can be segregated from homogeneous solid solutions of these alloys; as a consequence, the physical and chemical properties of alloys change dramatically. Therefore, it is of interest to study the properties, formation conditions, and existence boundaries of  $\sigma$  phases. This work studies the existence field of the  $\sigma$  phase in the Co–Cr–Ni–V quaternary at 800°C and vanadium percentages of 10 and 20 at %.

The binaries and ternaries of the Co–Cr–Ni–V quaternary have been well studied [1–10]. Phase equilibria, involving an FCC  $\gamma$  solid solution based on cobalt and nickel, a BCC  $\beta$  solid solution based on chromium and vanadium, and the  $\sigma$  phase, exist in all ternaries at temperatures near 800°C. In the Co–Cr–V and Co–Ni–V ternaries, the existence fields of  $\sigma$  phases extend from the Co–V side to the Co–Cr side [8] and Ni–V side [9], respectively. In the Co–Cr–Ni ternary, the homogeneity field of the  $\sigma$  phase penetrates the ternary system from the Co–Cr side to reach 18 at % nickel [7]. In the Cr–Ni–V ternary, it penetrates the ternary system from the Ni–V side to reach 32 at % chromium [10]. When vanadium percentages exceed 20 at %, intermetallic compounds  $\text{Co}_3\text{V}$ ,  $\text{Ni}_3\text{V}$ , and  $\text{Ni}_2\text{V}$  participate in phase equilibria. However, the homogeneity fields of these compounds in the ternaries are not large [9, 10].

In this work, we study and construct two sections of the Co–Cr–Ni–V isothermal tetrahedron at 10 and 20 at % vanadium. We synthesized 16 and 24 alloys, respectively. Inasmuch as our interest was focused on phase equilibria involving the  $\sigma$  phase, we strove to ensure that the compositions of alloys lay near the suggested homogeneity field of this phase. Alloys were alloyed in an electrical arc furnace in a purified argon atmosphere; then, they were annealed at 800°C for 1200 h with subsequent quenching to cold water. The

resulting samples were characterized using microstructure examination, X-ray powder diffraction (XRD), and electron probe microanalysis (EPMA).

X-ray powder diffraction analysis was carried out on a DRON-4 diffractometer using  $\text{CuK}_\alpha$  radiation. The STOE program was used to process X-ray diffraction patterns and calculate unit cell parameters. Table 1 compiles the results of XRD analysis.

Electron probe microanalysis was used to study alloys whose compositions fall into two- and three-phase fields. Compositions of constituent phases were determined on a JSM-820 (Joel) scanning electron microscope equipped with an AN 10/85S (Link) energy-dispersive attachment. The accelerating voltage on the cathode was 15 kV. The analytical lines used were the following characteristic lines:  $K_\alpha(\text{Co})$ ,  $K_\beta(\text{Cr})$ ,  $K_\alpha(\text{Ni})$ , and  $K_\beta(\text{V})$ . Table 2 displays EPMA results. In some cases, compositions were not determined for all equilibrium phases because of their low percentages and fine-grained structures. Reliable determinations were done only for the composition of the  $\sigma$  phase and the directions of two-phase tie-lines. We should note that equilibrium phase compositions in the quaternary are not always in the plane of the section.

The phase equilibrium character in the Ni–Co–Cr–V system containing 10 and 20 at % vanadium as determined by XRD and EPMA was verified by microstructure observation. The microstructure was observed with a Versamet-2 microscope under a magnification of 150–600. Chemical surface etching was used to provide phase contrast.

The sections of the Co–Cr–Ni–V isothermal tetrahedron containing 10 and 20 at % vanadium are displayed in Figs. 1a and 1b. When the system contains 10 at % vanadium, the section is on the whole similar to the structure of the Co–Cr–Ni ternary at 800°C as determined earlier [7]. The section is characterized by an extensive field of cobalt and nickel base solid solu-

**Table 1.** Phase composition and the unit cell parameters of constituent phases

| Alloy  | Phase composition       | FCC             | BCC               | $\sigma$ phase  |                 |
|--|-------------------------|-----------------|-------------------|-----------------|-----------------|
|  |                         | $a, \text{\AA}$ | $a, \text{\AA}$   | $a, \text{\AA}$ | $c, \text{\AA}$ |
| Co <sub>9</sub> Cr <sub>63</sub> Ni <sub>18</sub> V <sub>10</sub>      | FCC + BCC + $\sigma$    | 3.569(1)        | 2.883(1)          | 8.814(1)        | 4.546(2)        |
| Co <sub>9</sub> Cr <sub>58</sub> Ni <sub>22.5</sub> V <sub>10</sub>    | FCC + BCC               | 3.577(1)        | 2.888(1)          | –               | –               |
| Co <sub>13.5</sub> Cr <sub>54</sub> Ni <sub>22.5</sub> V <sub>10</sub> | FCC + BCC + $\sigma$    | 3.570(1)        | 2.888(1)          | 8.820(1)        | 4.538(1)        |
| Co <sub>13.5</sub> Cr <sub>58.5</sub> Ni <sub>18</sub> V <sub>10</sub> | FCC + BCC + $\sigma$    | 3.567(1)        | 2.884(1)          | 8.819(2)        | 4.552(2)        |
| Co <sub>13.5</sub> Cr <sub>63</sub> Ni <sub>13.5</sub> V <sub>10</sub> | BCC + $\sigma$          | –               | 2.886(1)          | 8.820(2)        | 4.569(2)        |
| Co <sub>18</sub> Cr <sub>58.5</sub> Ni <sub>13.5</sub> V <sub>10</sub> | BCC + $\sigma$          | –               | 2.883(1)          | 8.818(2)        | 4.550(2)        |
| Co <sub>18</sub> Cr <sub>54</sub> Ni <sub>18</sub> V <sub>10</sub>     | BCC + $\sigma$          | –               | –                 | 8.806(2)        | 4.548(2)        |
| Co <sub>22.5</sub> Cr <sub>49.5</sub> Ni <sub>18</sub> V <sub>10</sub> | FCC + $\sigma$          | 3.575(1)        | –                 | 8.805(2)        | 4.543(2)        |
| Co <sub>22.5</sub> Cr <sub>54</sub> Ni <sub>13.5</sub> V <sub>10</sub> | $\sigma$ phase          | –               | –                 | 8.795(1)        | 4.549(2)        |
| Co <sub>22.5</sub> Cr <sub>63</sub> Ni <sub>4.5</sub> V <sub>10</sub>  | BCC + $\sigma$          | –               | 2.885(1)          | 8.819(1)        | 4.549(1)        |
| Co <sub>27</sub> Cr <sub>58.5</sub> Ni <sub>4.5</sub> V <sub>10</sub>  | BCC + $\sigma$          | –               | 2.885(1)          | 8.819(1)        | 4.550(1)        |
| Co <sub>27</sub> Cr <sub>49</sub> Ni <sub>13.5</sub> V <sub>10</sub>   | $\sigma$ phase          | –               | –                 | 8.786(1)        | 4.541(1)        |
| Co <sub>31.5</sub> Cr <sub>45</sub> Ni <sub>13.5</sub> V <sub>10</sub> | FCC + $\sigma$          | 3.564(1)        | –                 | 8.785(2)        | 4.533(1)        |
| Co <sub>31.5</sub> Cr <sub>54</sub> Ni <sub>4.5</sub> V <sub>10</sub>  | $\sigma$ phase          | –               | –                 | 8.781(2)        | 4.538(1)        |
| Co <sub>40.5</sub> Cr <sub>45</sub> Ni <sub>4.5</sub> V <sub>10</sub>  | $\sigma$ phase          | –               | –                 | 8.760(2)        | 4.537(2)        |
| Co <sub>45</sub> Cr <sub>40.5</sub> Ni <sub>4.5</sub> V <sub>10</sub>  | FCC + $\sigma$          | 3.564(1)        | –                 | 8.773(1)        | 4.544(1)        |
| Co <sub>5</sub> Cr <sub>5</sub> Ni <sub>70</sub> V <sub>20</sub>       | FCC + Ni <sub>3</sub> V | 3.559(1)        | Ni <sub>3</sub> V | 3.543(1)        | 7.202(4)        |
| Co <sub>5</sub> Cr <sub>15</sub> Ni <sub>70</sub> V <sub>20</sub>      | FCC                     | 3.554(1)        | –                 | –               | –               |
| Co <sub>5</sub> Cr <sub>25</sub> Ni <sub>70</sub> V <sub>20</sub>      | FCC + BCC + $\sigma$    | 3.556(1)        | 2.890(1)          | Very little     |                 |
| Co <sub>20</sub> Cr <sub>15</sub> Ni <sub>45</sub> V <sub>20</sub>     | FCC + $\sigma$          | 3.574(1)        | –                 | 8.801(1)        | 4.536(1)        |
| Co <sub>35</sub> Cr <sub>10</sub> Ni <sub>35</sub> V <sub>20</sub>     | FCC + Co <sub>3</sub> V | 3.570(1)        | Co <sub>3</sub> V | 5.012(3)        | 12.18(2)        |
| Co <sub>25</sub> Cr <sub>25</sub> Ni <sub>30</sub> V <sub>20</sub>     | FCC + $\sigma$          | 3.559(1)        | –                 | 8.828(3)        | 4.547(2)        |
| Co <sub>20</sub> Cr <sub>30</sub> Ni <sub>30</sub> V <sub>20</sub>     | FCC + $\sigma$          | 3.553(1)        | –                 | 8.832(1)        | 4.555(1)        |
| Co <sub>10</sub> Cr <sub>40</sub> Ni <sub>30</sub> V <sub>20</sub>     | FCC + BCC + $\sigma$    | 3.5247          | 2.894(2)          | 8.859(2)        | 4.554(1)        |
| Co <sub>5</sub> Cr <sub>45</sub> Ni <sub>30</sub> V <sub>20</sub>      | FCC + BCC + $\sigma$    | 3.523(1)        | 2.8957            | Very little     |                 |
| Co <sub>30</sub> Cr <sub>25</sub> Ni <sub>25</sub> V <sub>20</sub>     | FCC + $\sigma$          | 3.526(1)        | –                 | 8.805(2)        | 4.560(2)        |
| Co <sub>25</sub> Cr <sub>30</sub> Ni <sub>25</sub> V <sub>20</sub>     | FCC + $\sigma$          | 3.529(1)        | –                 | 8.805(1)        | 4.556(2)        |
| Co <sub>15</sub> Cr <sub>40</sub> Ni <sub>25</sub> V <sub>20</sub>     | $\sigma$ phase          | –               | –                 | 8.838(1)        | 4.557(1)        |
| Co <sub>10</sub> Cr <sub>45</sub> Ni <sub>25</sub> V <sub>20</sub>     | FCC + BCC + $\sigma$    | 3.558(1)        | 2.888(1)          | 8.834(1)        | 4.569(1)        |
| Co <sub>50</sub> Cr <sub>15</sub> Ni <sub>15</sub> V <sub>20</sub>     | FCC + $\sigma$          | 3.5524          | –                 | Very little     |                 |
| Co <sub>40</sub> Cr <sub>25</sub> Ni <sub>15</sub> V <sub>20</sub>     | FCC + $\sigma$          | 3.537(1)        | –                 | 8.817(1)        | 4.549(1)        |
| Co <sub>35</sub> Cr <sub>30</sub> Ni <sub>15</sub> V <sub>20</sub>     | FCC + $\sigma$          | 3.542(1)        | –                 | 8.811(2)        | 4.560(2)        |
| Co <sub>25</sub> Cr <sub>40</sub> Ni <sub>15</sub> V <sub>20</sub>     | $\sigma$ phase          | –               | –                 | 8.822(1)        | 4.550(1)        |
| Co <sub>20</sub> Cr <sub>45</sub> Ni <sub>15</sub> V <sub>20</sub>     | BCC + $\sigma$          | –               | 2.849(1)          | 8.835(7)        | 4.558(4)        |
| Co <sub>10</sub> Cr <sub>55</sub> Ni <sub>15</sub> V <sub>20</sub>     | BCC + $\sigma$          | –               | 2.8957            | 8.841(1)        | 4.555(1)        |
| Co <sub>70</sub> Cr <sub>5</sub> Ni <sub>5</sub> V <sub>20</sub>       | FCC + Co <sub>3</sub> V | 3.5244          | Co <sub>3</sub> V | 4.979(1)        | 12.296          |
| Co <sub>50</sub> Cr <sub>25</sub> Ni <sub>5</sub> V <sub>20</sub>      | FCC + $\sigma$          | 3.5296          | –                 | 8.802(1)        | 4.543(1)        |
| Co <sub>40</sub> Cr <sub>35</sub> Ni <sub>5</sub> V <sub>20</sub>      | $\sigma$ phase          | –               | –                 | 8.804(2)        | 4.541(2)        |
| Co <sub>30</sub> Cr <sub>45</sub> Ni <sub>5</sub> V <sub>20</sub>      | $\sigma$ phase          | –               | –                 | 8.831(1)        | 4.551(1)        |
| Co <sub>20</sub> Cr <sub>55</sub> Ni <sub>5</sub> V <sub>20</sub>      | BCC + $\sigma$          | –               | 2.894(1)          | 8.856(3)        | 4.563(1)        |

**Table 2.** Electron probe microanalysis data for Co–Cr–Ni–V alloys

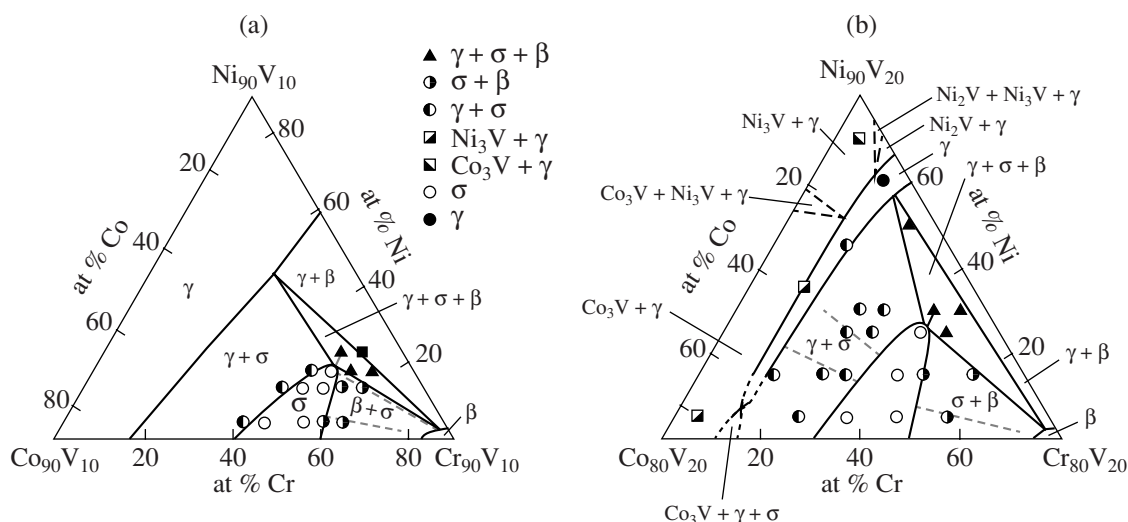
| As-batch composition of alloy, at % |      |      |    | Phase composition              | Constituent phase     | Composition of the constituent phase, at % |        |       |       |
|-------------------------------------|------|------|----|--------------------------------|-----------------------|--|--------|-------|-------|
| Co                                  | Cr   | Ni   | V  |                                |                       | Co   | Cr     | Ni    | V     |
| Alloys containing 10 at % vanadium  |      |      |    |                                |                       |  |        |       |       |
| 13.5                                | 54   | 22.5 | 10 | $\beta + \gamma + \sigma$      | $\sigma$ phase        | 16.08                                      | 54.14  | 19.0  | 10.78 |
| 13.5                                | 63   | 13.5 | 10 | $\beta + \sigma$               | $\sigma$ phase        | 16.13                                      | 54.33  | 17.24 | 12.3  |
| 22.5                                | 63   | 4.5  | 10 | $\beta + \sigma$               | $\sigma$ phase        | 24.18                                      | 60.301 | 5.64  | 9.87  |
| 22.5                                | 49.5 | 18   | 10 | $\gamma + \sigma$              | $\sigma$ phase        | 21.7                                       | 50.6   | 16.5  | 11.2  |
| 31.5                                | 45   | 13.5 | 10 | $\gamma + \sigma$              | $\sigma$ phase        | 29.05                                      | 47.6   | 12.5  | 10.85 |
| Alloys containing 20 at % vanadium  |      |      |    |                                |                       |  |        |       |       |
| 35                                  | 10   | 35   | 20 | $\text{Co}_3\text{V} + \gamma$ | $\text{Co}_3\text{V}$ | 42.9                                       | 8.0    | 19.2  | 28.9  |
| 10                                  | 40   | 30   | 20 | $\beta + \gamma + \sigma$      | $\sigma$ phase        | 11.4                                       | 39.7   | 27.1  | 21.8  |
| 30                                  | 25   | 25   | 20 | $\gamma + \sigma$              | $\sigma$ phase        | 25.1                                       | 35.7   | 20.8  | 18.4  |
| 35                                  | 30   | 15   | 20 | $\gamma + \sigma$              | $\sigma$ phase        | 34.0                                       | 34.5   | 12.9  | 18.6  |
|                                     |      |      |    |                                | $\gamma$ phase        | 35.4                                       | 18.3   | 23.1  | 22.2  |
| 20                                  | 55   | 5    | 20 | $\beta + \sigma$               | $\sigma$ phase        | 23.62                                      | 50.18  | 5.72  | 20.5  |

tion. Addition of vanadium leads to some increase in the  $\sigma$  homogeneity field in the quaternary; the maximal nickel solubility is 20.5 at %. The  $\sigma$  homogeneity field is directed toward the metastable  $\sigma$  phase of the Cr–Ni–V face.

The cobalt and nickel solubility in the BCC phase is insignificant. X-ray powder diffraction (Table 1) shows that the unit cell parameters of the BCC phase in all two-phase and three-phase samples remain almost constant and close to the unit cell parameter of pure chromium (2.8888 Å).

The position of the equilibrium BCC + FCC +  $\sigma$  three-phase field was determined with reference to the intensity ratio of reference lines in the X-ray diffraction patterns of  $\text{Co}_{13.5}\text{Cr}_{54}\text{Ni}_{22.5}$ ,  $\text{Co}_{13.5}\text{Cr}_{58.5}\text{Ni}_{18}$ , and  $\text{Co}_9\text{Cr}_{63}\text{Ni}_{18}$  three-phase samples and the nickel solubility in the  $\sigma$  phase determined by EPMA (Table 2).

The section of the Co–Cr–Ni–V system containing 20 at % vanadium is depicted in Fig. 1b. In the chromium-rich region, this section is similar to the section containing 10 at % vanadium. The BCC solid solution has an insignificant homogeneity field; the unit cell parameters of the BCC phase are close to the unit cell

**Fig. 1.** Sections of the Co–Cr–Ni–V quaternary at 800°C with vanadium atom percentages (at %) of (a) 10 and (b) 20.

parameters of the relevant Cr–V alloys. The nickel solubility in the  $\sigma$  phase is  $\sim 27$  at %. There is also an extensive homogeneous field of the  $\gamma$  phase (an FCC structure), which penetrates up to 50–55 at % Co into the quaternary from the Cr–Ni–V side. The penetration depth of the FCC phase into the isothermal tetrahedron for 20 at % vanadium was judged from XRD data for the  $\text{Co}_{20}\text{Cr}_{15}\text{Ni}_{45}\text{V}_{20}$  and  $\text{Co}_{50}\text{Cr}_{15}\text{Ni}_{15}\text{V}_{20}$  alloys. The X-ray diffraction patterns of these samples were identical, each containing two sets of reflections; the strongest lines were due to an FCC structure. The second phase  $\sigma$  was detected by the very weak reflections from its reference lines.

The position of the BCC + FCC +  $\sigma$  three-phase field was determined by EPMA and XRD of  $\text{Co}_5\text{Cr}_{25}\text{Ni}_{70}\text{V}_{20}$ ,  $\text{Co}_{10}\text{Cr}_{40}\text{Ni}_{30}\text{V}_{20}$ ,  $\text{Co}_5\text{Cr}_{45}\text{Ni}_{30}\text{V}_{20}$ , and  $\text{Co}_{10}\text{Cr}_{45}\text{Ni}_{25}\text{V}_{20}$  three-phase samples.

The ordering of the  $\gamma$  solid solution along the  $\text{Co}_{80}\text{V}_{20}$ – $\text{Ni}_{80}\text{V}_{20}$  side of the isoconcentration triangle generates  $\sigma$  +  $\text{Co}_3\text{V}$  and  $\gamma$  +  $\text{Ni}_3\text{V}$  two-phase fields.

The field of the  $\text{Ni}_3\text{V}$  +  $\text{Ni}_2\text{V}$  +  $\gamma$  three-phase equilibrium is depicted on the 20 at % vanadium section provisionally, on the basis of data on the Cr–Ni–V ternary [10]. The  $\text{Ni}_3\text{V}$  +  $\text{Co}_3\text{V}$  +  $\gamma$  three-phase field is depicted on the triangular diagram with reference to the X-ray diffraction study along the  $\text{Co}_3\text{V}$ – $\text{Ni}_3\text{V}$  section performed by Koester and Sperner [9]. Although Koester and Sperner [9] were mistaken in believing that the aforementioned compounds form continuous solid solutions, the unit cell parameter plots show a flex point

when  $\text{Ni} : \text{Co} = 3 : 1$ . This trend implies that the  $\text{Co}_3\text{V}$  +  $\text{Ni}_3\text{V}$  two-phase field indeed exists in this compositional region.

In summary, comparing the sections of the Co–Cr–Ni–V isothermal tetrahedron containing 10 and 20 at % vanadium, we have seen that an increase in vanadium percentage increases the existence field of the  $\sigma$  phase from 18 at % Ni [7] to 27 at % Ni.

## REFERENCES

1. Ishida, K. and Nishizawa, T., *Bull. Alloy Phase Diagrams*, 1990, vol. 11, p. 357.
2. Massalski, T.B., *Binary Alloy Phase Diagrams*, Ohio, 1986.
3. Smith, J.F., *J. Phase Equil.*, 1991, vol. 12, p. 324.
4. Nash, P., *Bull. Alloy Phase Diagrams*, 1986, vol. 7, p. 465.
5. Lee, B.-J., *Z. Metallkde*, 1992, vol. 83, p. 292.
6. Smith, J.F., Carlson, O.N., and Nash, P.G., in *Phase Diagrams of Binary Nickel Alloys*, Nash, P., Ed., Ohio, 1986, p. 361.
7. Zhmurko, G.P., Kabanova, E.G., Kuznetsov, V.N., and Leonov, A.V., *Vestn. Mosk. Univ., Ser. 2: Khim.*, 2008, vol. 49, p. 283.
8. Kuznetsov, V.N., Zhmurko, G.P., Toibaev, Zh.N., et al., *Vestn. Mosk. Univ., Ser. 2: Khim.*, 2001, vol. 42, p. 121.
9. Koester, W. and Sperner, F., *Z. Metallkd.*, 1957, vol. 43, p. 540.
10. Kodentsov, A.A., Dunaev, S.F., and Slusarenko, E.M., *J. Less-Common Met.*, 1987, vol. 135, p. 15.